

Journal of Materials Chemistry B

Accepted Manuscript



This is an *Accepted Manuscript*, which has been through the Royal Society of Chemistry peer review process and has been accepted for publication.

Accepted Manuscripts are published online shortly after acceptance, before technical editing, formatting and proof reading. Using this free service, authors can make their results available to the community, in citable form, before we publish the edited article. We will replace this *Accepted Manuscript* with the edited and formatted *Advance Article* as soon as it is available.

You can find more information about *Accepted Manuscripts* in the [Information for Authors](#).

Please note that technical editing may introduce minor changes to the text and/or graphics, which may alter content. The journal's standard [Terms & Conditions](#) and the [Ethical guidelines](#) still apply. In no event shall the Royal Society of Chemistry be held responsible for any errors or omissions in this *Accepted Manuscript* or any consequences arising from the use of any information it contains.

Cite this: DOI: 10.1039/c0xx00000x

www.rsc.org/xxxxxx

Gold-modified silver nanorod arrays for SERS-based immunoassays with improved sensitivity

Chunyuan Song,^{*a,b,c} Jing Chen,^{c,d} Yiping Zhao,^{b,c} and Lianhui Wang^{*a}*Received (in XXX, XXX) Xth XXXXXXXXXX 20XX, Accepted Xth XXXXXXXXXX 20XX*

DOI: 10.1039/b000000x

In sandwich SERS immunoassays, the SERS-active substrate plays a central role to gain the detection sensitivity. Silver nanorod (AgNR) arrays fabricated by oblique angle deposition (OAD) provide superior analytical qualities and have been demonstrated as excellent SERS substrates. This work reports highly sensitive sandwich immunoassays performed on the OAD-AgNR substrates for the first time, utilizing 4-MBA-labeled immuno-Au nanoparticles (Im-AuNPs) as SERS tags. The aligned AgNR arrays were first deposited on glass slides by OAD, and surface-modified with gold (Au) using chloroauric acid solution *via* a galvanic replacement reaction. Immunoassays executed on both AgNR arrays and Au-modified AgNR arrays show higher detection sensitivity compared to that performed on self-assembled silver nanoparticles substrates. Though the AgNRs demonstrate better SERS activity than Au-modified AgNRs, the immunoassay performed on the Au-modified AgNRs exhibits a higher sensitivity. Further characterization with scanning electron microscopy and fluorescence spectroscopy show that the improved sensitivity can be attributed to an increased number of Im-AuNPs that are specifically captured on the Au-modified nanorods surface and their more uniform distribution. Concentration-dependent SERS spectra of human IgG on the Au-modified AgNR arrays reveal a good linear response range of 100 fg/mL to 100 ng/mL, with a LOD of 2.5 fg/mL.

1 Introduction

Immunoassays based on surface enhanced Raman scattering (SERS) are a type of specific biochemical test for target substances in complex mixtures, and have attracted wide attention in a variety of fields, including proteomics, drug delivery, food safety, environmental science, health care, and homeland security¹⁻⁸. One of the most widely adopted formats of immuno-SERS detection is the standard antibody-based sandwich assay⁹. This strategy generally involves three steps: i) immobilization of capture antibodies onto a supporting substrate; ii) specific capture of analytes from a complex solution onto the substrate through the immobilized antibodies; and iii) exposing the substrate to analyte-specific SERS tags. Generally, a SERS tag is a noble metal nanoparticle labeled with the specific antibody and a Raman reporter, which can be anchored onto the supporting substrate *via* the test analyte. Once the sandwich structure is formed, the SERS signal from the Raman reporter can be detected qualitatively or quantitatively.

In recent years, SERS-based immunoassays have been used to specifically and sensitively detect a number of targets, including virus DNAs¹, cancer markers¹⁰, vitamin D3¹¹, proteins¹², kinases¹³, bacteria¹⁴, *etc.* By far, many sensitive SERS tags based on various metal nanostructures have been proposed. These SERS tags ranged from composite organic-

inorganic nanoparticles¹⁵, core-shell structures^{16, 17}, hollow nanospheres^{10, 18}, aggregates¹⁹ to organic-metal-quantum dot hybrid nanoparticles²⁰. On the other hand, SERS-active substrates also play an important role in detection sensitivity, since many SERS "hot spots" may emerge at the junction of the SERS tags and SERS-active supporting substrate in a sandwich structure²¹⁻²³. Such a discovery opens up enormous opportunities to utilize various available SERS-active substrates in sandwich SERS immunoassays for ultrasensitive detection.

In particular, aligned Ag nanorod (AgNR) arrays fabricated by the oblique angle deposition (OAD) technique have demonstrated as highly uniform and ultra-sensitive SERS substrates^{24, 25}. SERS enhancement factors of greater than 10⁸ have been achieved with the AgNR substrates, and these substrates have been successfully used to detect different chemical and biological agents²⁶. Previously we have demonstrated that modification of the AgNR surface with a layer of gold (Au) using galvanic replace reaction (GRR) for 20 min can improve the stability and sensitivity of SERS detection, which is valuable in real-world sensing applications²⁷. Combined with the nanoparticle SERS tags, these highly stable AgNR substrates are expected to provide additional SERS enhancement and improve the overall detection sensitivity in SERS-based sandwich immunoassays.

Here we report a sandwich SERS immunoassay using the

AgNR arrays fabricated by OAD as the supporting substrate for the first time. Anti-human IgG antibodies were immobilized onto AgNR or Au-modified AgNR substrates, which are used to capture the analytes and then immunologically recognize the SERS tags for the specific detection of human IgGs. The SERS response of the immunoassays based on AgNRs and Au-modified AgNRs are compared, and the limit of detection (LOD) is assessed using the concentration-dependent SERS response.

2 Experimental section

2.1 Chemicals

The evaporation source materials, silver (99.999%) and titanium (99.995%) were purchased from Kurt J. Lesker (Jefferson Hills, PA, USA). Hydrogen tetrachloroaurate trihydrate ($\text{HAuCl}_4 \cdot 3\text{H}_2\text{O}$, 99.999%) and 4-mercaptobenzoic acid (4-MBA) were acquired from Sigma-Aldrich (St. Louis, MO, USA). Trisodium citrate ($\text{Na}_3\text{C}_6\text{H}_5\text{O}_7 \cdot 2\text{H}_2\text{O}$) was obtained from Sinopharm Chemical Reagent CO., Ltd (Shanghai, China). Human-IgG, goat anti-human IgG, FITC-labeled goat anti-human IgG, and bovine serum albumin (BSA) were purchased from Nanjing KeyGEN Biotechnology CO., Ltd (Nanjing, Jiangsu, China). All chemicals and materials were used as received. All protein samples were diluted in borate buffer solution (BBS, 2 mM, pH = 9). Tris-buffered saline (TBS, 10 mM Tris, 150 mM NaCl, pH = 7~8) and TBST buffer solution (TBS + 0.1% Tween 20, pH = 7~8) were used as washing buffers.

2.2 Fabrication and surface-functionalization of AgNR and Au-modified AgNR substrates

The AgNR substrates were prepared through the OAD process in a custom-built electron beam evaporation system^{24, 28}. Before deposition, clean glass slides (9 mm × 9 mm) were mounted into the deposition chamber with the substrate normal anti-parallel to the incident vapor direction. The entire evaporation process was conducted under high vacuum conditions ($< 3 \times 10^{-6}$ Torr), and the deposition rate and thickness of the deposited films were monitored by a quartz crystal microbalance directly facing the vapor. A 20-nm layer of Ti was first deposited at a rate of 0.2 nm/s, followed by a 200-nm Ag film deposited at 0.3 nm/s. The substrate normal was then rotated to 86° relative to the incident vapor direction, and a final 2000-nm layer of AgNRs was deposited at a rate of 0.3 nm/s. Details of the deposition configuration can be found in the Electronic Supplementary Information (ESI†) Fig. S1.

The Au-modified AgNR arrays were prepared *via* GRR as described in our previous work²⁷. Briefly, the as-deposited AgNR substrates were completely immersed in 2 mL of 1 mM chloroaurate acid solution in a test tube for 20 min, followed by thorough rinsing with DI water and drying with nitrogen. Both as-deposited AgNR and Au-modified AgNR substrates were sealed in plastic petri dishes for later use.

To prepare the capture substrates, 2 μL of 2 mg/mL goat anti-human IgG antibody (diluted in BBS) was pipetted onto the as-deposited AgNR or Au-modified AgNR substrates. Immobilization of antibodies was carried out at 4°C for 12 h in a chamber with a relative humidity of 65% ~ 75%. This step resulted in a layer of antibodies on the substrates through the

ionic and hydrophobic interactions as well as Ag-S or Au-S binding between the substrate and sulfur-containing amino acids of the antibodies⁵. The substrates were then rinsed with TBS and DI water three times to remove the residual antibodies, and then exposed to the blocking buffer containing 3% BSA (in BBS) for 3 h at room temperature to block any free binding sites on the substrate surface. After thoroughly rinsing with TBST, TBS, and DI water, the functionalized substrates were dried with nitrogen and stored at 4°C for the immuno-SERS assays.

2.3 Preparation of Im-AuNPs

The SERS tags, *i.e.*, 4-MBA-labeled immuno-Au nanoparticles (Im-AuNPs), were prepared by functionalizing AuNPs with anti-human IgG antibodies and a Raman reporter, 4-MBA. Colloidal gold was prepared following the procedure developed by Frens²⁹. Briefly, 4 mL of 1% trisodium citrate in aqueous solution was added into 100 mL of 10^{-4} g/mL HAuCl_4 solution immediately after boiling, and the mixture was vigorously stirred for 20 min until the color turned red by the AuNPs. Then 0.2 μL of 1 mM 4-MBA (diluted in ethanol) was mixed with 1 mL cooled gold colloid under vigorous stirring to allow the Raman reporter molecules to be anchored onto the AuNPs *via* thiol-gold interactions. The mixture was allowed to continue reacting overnight and excess 4-MBA molecules were removed from the labeled AuNPs through three cycles of centrifugation at 10000 rpm for 30 min and rinsing with BBS buffer. After decanting the clear supernatant, the loose red sediment was resuspended in 1 mL of BBS under ultrasonic agitation. In the third step, 10 μL of 2 mg/mL goat anti-human IgG antibodies were added to 1 mL of the 4-MBA-labeled AuNPs and allowed to incubate at 4°C for 2 h. After two centrifugation-rinsing cycles (each at 10000 rpm for 30 min), the resultant Im-AuNPs were incubated with 10 μL of 3% BSA for 1 h at room temperature to block any free binding sites on the surface. After centrifuging at 10000 rpm for 30 min and rinsing with BBS twice, the Im-AuNPs were resuspended in 0.5 mL of BBS and stored at 4°C.

2.4 Immunoassay protocol

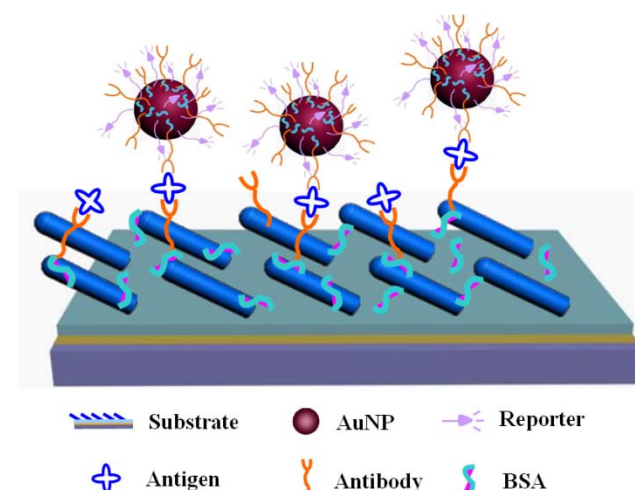


Fig.1 Schematic map of the sandwiched immuno-SERS assay performed on aligned AgNR substrates.

The immuno-SERS assays were carried out in a standard sandwich immunoassay format as illustrated in Fig. 1. First, 20

μL of 100 $\mu\text{g}/\text{mL}$ human-IgGs were pipetted onto antibody-modified AgNR or Au-modified AgNR substrates (*i.e.* capture substrate), which were then incubated for 2 h at 37°C. Then the substrates were sequentially rinsed by TBST, TBS, and DI water. The immune SERS tags were applied to the sample spots, and allowed to incubate with the capture substrates for 2 h at 4°C and 65% ~ 70% relative humidity. The substrates were then successively rinsed with TBST, TBS and DI water, and finally dried by nitrogen for immediate SERS detection.

2.5 Instrumentation

A UV-Vis spectrophotometer (UV-3600, Shimadzu, Japan) was used to monitor the optical properties of Au and Ag nanostructures. Transmission electron microscope (TEM) (FEI, Tecnai 20) was used to characterize the morphology of AuNPs. Scanning electron microscopy (SEM) images were obtained by a field emission scanning electron microscopy (FESEM) (Sirion200, FEI, Holand). A high speed centrifuge (2-16PK, Sigma, Germany) was used for sample preparation. All SERS spectra were acquired at an excitation wavelength of 633 nm and a laser power of 2.3 mW, through a 10 \times objective lens (NA = 0.4) and an Andor shamrock spectrograph (Shamrock, Andor, UK). The width of the slit was 100 μm , and a grating of 1200 lines/mm was used to disperse the scattered light. Unless otherwise stated, all the spectra reported here were obtained using a single 30 s accumulation.

3 Results and discussion

3.1 Characterization of AgNR and Au-modified AgNR arrays

The top view SEM images of AgNR and Au-modified AgNR arrays are shown in Figure 2a and 2b, respectively. Tilted, aligned rods with a wide range of morphologies, such as corrugations, bifurcations, protrusions, and other irregular morphologies, are found to randomly distribute on the as-deposited AgNR substrate (Fig. 2a). The average diameter of the AgNRs measured at the tips is approximately 80 nm, and the average rod length is approximately 1000 nm. The tilting angle (as shown in the ESI† Fig. S2) is about $77 \pm 1^\circ$ and the density of nanorods is estimated to be 15 rods/ μm^2 . After modification with Au, significant changes in morphology were observed on the AgNRs (Fig. 2b). During GRR, AuCl_4^- ions are reduced to Au atoms, and Ag^+ ions are released into the solution³⁰. The reduced Au atoms are then epitaxially deposited onto the AgNRs, adapting the morphology of the original Ag template forming Au-Ag alloy layer, ultimately expanding the rod diameter to approximately 210 nm. In the meantime, some smaller and thinner AgNRs break into fragments and are removed from the substrate during subsequent washing steps²⁷, which decreases the density of the Au-modified AgNRs to approximately 9 rods/ μm^2 . Despite the decreased density of nanorods on the substrate, the gaps between individual nanorods become smaller due to the increase of nanorod diameter. Moreover, the underlying Ag film is also exposed to chloroaurate acid solution, which is likely to lead to further Au deposition onto the bottom of the gap space between the nanorods and further reduce the volume of the gap space.

The SERS properties of these two types of substrates were characterized using a Raman reporter, 4-MBA. Before SERS

measurements, the substrates were soaked in 2 mL of 1 mM 4-MBA for 30 min, and then rinsed thoroughly with water and dried with nitrogen. Fig. 2c shows the SERS spectra of 4-MBA collected on the AgNR and Au-modified AgNR substrates. The characteristic SERS peaks of 4-MBA at 1080 cm^{-1} and 1587 cm^{-1} indicate that both substrates are SERS-active. After Au modification, the SERS enhancement of the substrate decreases as the SERS intensity of the 1080 cm^{-1} 4-MBA peak decays to less than 20% of that obtained on the bare AgNR substrate. This observation is consistent with our previous finding on the Au-modified AgNR substrates in which the GRR reaction time was found to be related to the SERS activity of the modified substrates²⁷. Previous experimental data and analysis indicate that the main cause for the decreased SERS enhancement after Au modification is the compositional changes on the substrate, as a large number of Ag atoms are displaced by Au. Because the SERS activity depends strongly on the substrate material, and the SERS enhancement ability of Au is in general 100 times lower than that of Ag³¹, increasing the percentage of Au in the substrate material decreases the SERS activity of the Au-modified substrates. In spite of decreased SERS enhancement, both bare AgNR and Au-modified AgNR substrates maintain good signal reproducibility. The peak intensities at 1587 cm^{-1} and 1080 cm^{-1} collected from multiple locations on the substrates exhibit relative standard deviations (RSDs) of 5.5% and 6.7% on bare AgNR substrates, and 5.5% and 6.4% on Au-modified AgNR substrates, respectively (ESI† Fig. S3).

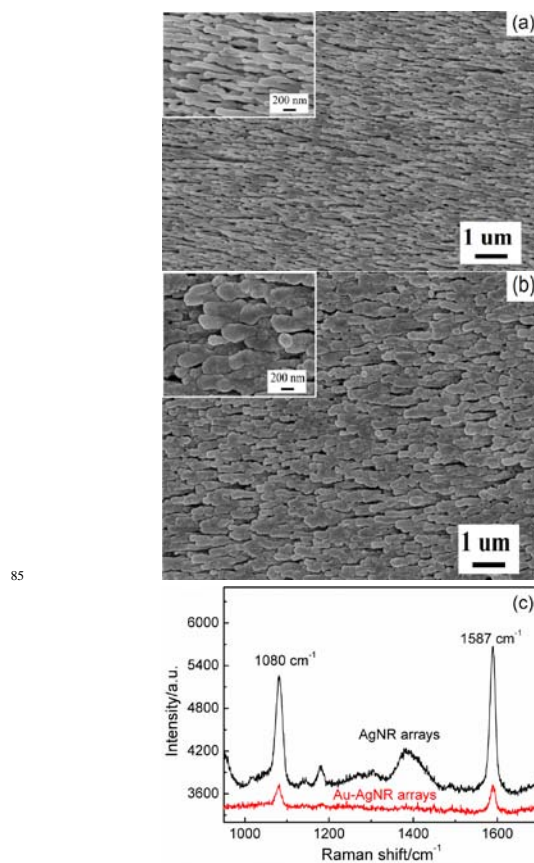


Fig.2 Top view SEM images of the AgNR array (a) and Au-modified AgNR array (b), and the SERS spectra of 4-MBA acquired on the AgNR array and Au-modified AgNR array (c).

3.2 Characterization of the Im-AuNPs

The average diameter of the synthesized AuNPs is approximately 18 nm as shown in the TEM image in the ESI† Fig. S4. The monodispersed Au colloid displays a red color and has a localized surface plasma resonance (LSPR) peak at 519 nm (black curve in the ESI† Fig. S5). When the AuNPs were labeled with 4-MBA, the refractive index of the medium surrounding the nanoparticles changes due to the immobilized 4-MBA layer^{32, 33}, which leads to a slight red shift of the LSPR peak to 521 nm (red curve in the ESI† Fig. S5). The subsequent coating of goat anti-human IgG antibodies further shifts the LSPR peak to 526 nm (blue curve in the ESI† Fig. S5). As discussed in Reference²¹, Au colloids are stable in solution due to the electrostatic repulsion between their charged surfaces. When the 4-MBA molecules adsorb covalently to the particle surface, the citrate layers on the AuNPs are replaced by the S-Au bond. Low coverage of reporters affects the surface charges slightly, and the interparticle distances are still substantially greater than the average particle diameter³⁴. The colloids mainly exhibit the extinction characteristics of the dispersed particles, which indicates a well-preserved monodispersity of the Im-AuNPs.

3.3 Immunoassay

In this proposed immuno-SERS assay, the target antigen (human-IgG) is indirectly detected both qualitatively and quantitatively by the characteristic SERS signal of the Raman reporter, 4-MBA. As shown in Fig. 3a, on the AgNR substrates, the target sample, human-IgG (curve 1), exhibit distinct SERS spectral features from the blank control, BSA (curve 2), as pronounced peaks of 4-MBA at 1080 cm⁻¹ and 1587 cm⁻¹ are only identifiable in the target spectra. Similar results are obtained on the Au-modified AgNR substrates (curve 3 and 4 in Fig. 3a). In both cases, only negligible SERS signal of 4-MBA is observed on the blank control, which suggests that most nonspecifically adsorbed Im-AuNPs have been removed from the capture substrates after thorough rinsing. In addition, the SERS spectra acquired from six different locations on the substrates are highly reproducible with a low RSD (5.0%) at 1080 cm⁻¹ (ESI† Fig. S6).

To evaluate the effect of the capture AgNR substrates on the sensitivity of the sandwich immuno-SERS assay, an additional experiment was performed following the same protocol except that the AgNR arrays were replaced by a film of silver nanoparticles (AgNPs) which we reported previously^{21, 35}. As shown in curve 5 in Fig. 3a, the characteristic peaks of 4-MBA are found at significantly lower intensities compared to those obtained on the AgNR substrates at the same target concentration. The baseline-corrected SERS spectra of human-IgGs detected on the AgNPs film, AgNR array, and Au-modified AgNR array substrates (Fig. 3b) and the corresponding 4-MBA peak intensities (Table 1) demonstrate that the signal intensity of the immunoassay is highest when performed on the Au-modified AgNR substrates, followed by the AgNR substrates, both of which far exceed that conducted on the AgNP substrates. The SERS signal obtained on Au-modified AgNR substrates is approximately 1.42-1.46 and 5.73-6.26 times as strong as that on the AgNR substrates and AgNP films, respectively.

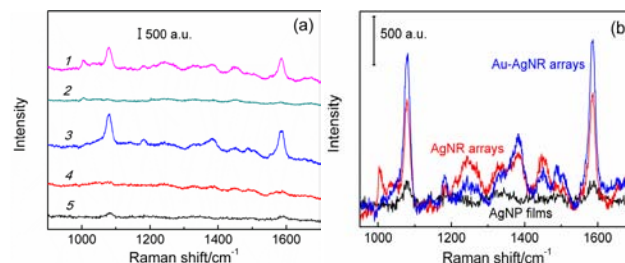


Fig.3 (a) SERS-based immunoassays on different substrates. Spectra 1 and 2 represent the SERS detections of human IgG (target) and BSA (control) on AgNR substrates, respectively. Spectra 3 and 4 are the SERS detections of human IgG and BSA on Au-modified AgNR substrates, respectively. Spectrum 5 represents human IgG on a self-assembled AgNP films. (b) Baseline-corrected SERS detections of human IgG obtained on AgNP films, AgNR arrays, and Au-modified AgNR substrates.

Table 1. SERS intensities of the immunoassay collected on three different SERS-active substrates. The spectra were subject to baseline correction before peak intensities were estimated.

SERS substrate	Peak intensity (a.u.)	
	1080 cm ⁻¹	1587 cm ⁻¹
AgNP films	274	273
AgNR arrays	1105	1172
Au-modified AgNR arrays	1570	1710
$I_{Au-AgNRs} / I_{AgNRs}$	1.42	1.46
$I_{Au-AgNRs} / I_{AgNPs}$	5.73	6.26

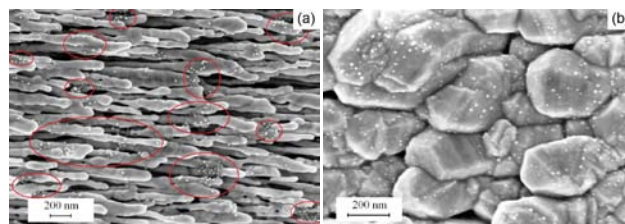


Fig.4 SEM images of the AgNR array and Au-modified AgNR array obtained after the immunoassay. The circled areas indicate regions with high AuNPs density.

Though in previous studies, the AgNR arrays have demonstrated higher SERS activity than the Au-modified AgNRs for direct molecular analysis, the results obtained in this SERS-based immunoassay are quite different. To explain this observation, the distributions of Im-AuNPs on these two types of substrates were investigated first, as the intensity of SERS signal depends strongly on the amount of the SERS tags on the substrates. Fig. 4a and 4b show the SEM images of the AgNR array and Au-modified AgNR array taken after the immunoassay, respectively. The scattered bright spots on the surface of the nanorods represent the Im-AuNPs specifically captured by human-IgGs through the antigen-antibody interaction. Most Im-AuNPs on the AgNRs are split up into relatively discrete clusters across a relatively wide area as marked by the red circles. The distribution of Im-AuNPs clearly exhibits non-uniformity, with the number of particles ranging from several to dozens of nanoparticles in clusters. The overall surface density is estimated

to be 65.5 particles/ μm^2 . In contrast, the Im-AuNPs on the Au-modified AgNR array display a much higher uniformity, as shown in Fig. 4b. The surface density of AuNPs adsorbed on the Au-modified AgNRs is approximately 90.6 particles/ μm^2 , which is about 1.4 times as many as that on AgNR substrate. Such a distribution difference of Im-AuNPs on the two types of substrates can be attributed to two factors: the wetting properties and the biocompatibility of the substrates. Our previous studies indicate that the water contact angle on the AgNR surface changes from $\sim 50^\circ$ to $\sim 30^\circ$ when its surface was modified with Au through 20 min of GRR. Au modification makes the surface more hydrophilic, which favors a more uniform layer of immobilized antibodies on the substrate. On the other hand, gold is generally considered as a more biocompatible substrate for protein immobilization. These two factors have likely led to a higher adsorption rate of antibodies and more uniform distribution of AuNPs on the Au-modified substrate, allowing for the capture of more human-IgGs from the sample solution onto the substrate.

To quantify the adsorption of antibodies on the two substrates, we conducted a simple experiment in which the anti-human IgGs were replaced by FITC-labeled goat anti-human IgG antibodies and allowed to adsorb onto the AgNRs and Au-modified AgNRs. After soaking for 12 h at 4°C , the substrates were removed from the antibody solution and rinsed with BBS. Both the antibody solution and rinsing buffer were collected and examined by fluorescence spectroscopy (FLS 900, Edinburgh, UK). As can be found in the ESI† Fig. S7, the fluorescence intensities at the 519 nm FITC peak are 79960 and 74470 counts for the residual soak solutions used to modify the AgNR and Au-modified AgNR substrates, respectively. As a reference, the unused FITC-labeled antibody solution shows a fluorescence intensity of 104400 counts. Thus, assuming each antibody carries the same amount of FITC molecules, the amount ratio κ of antibodies immobilized on the two types of substrates can be estimated using the fluorescence signal of the residual soaking solutions as follows,

$$\kappa = \frac{I - I_{s-Ag}}{I - I_{s-Au}} = 1.23$$

where I , I_{s-Ag} , and I_{s-Au} represent the 519 nm peak intensities detected from unused FITC-labeled goat anti-human IgG solution, and the residual solutions used to soak the AgNR and Au-modified AgNR substrates, respectively. This calculation indicates that the amount of antibodies anchored onto the Au-modified AgNR substrate is 1.23 times higher in relative to those on the AgNR substrate, which confirms that the Au-modified surface has a higher adsorption rate for anti-human IgGs compared to bare AgNRs.

Improved antibody immobilization can be considered as a major contributor for the higher sensitivity observed on the Au-modified AgNR substrates, since the increased number of immobilized Im-AuNPs also results in stronger 4-MBA signal. It is worth noting that though high local density is also found in some regions on the AgNR substrate, the average density of AuNPs over a larger area plays a more important role in the SERS detection, as the sampling dimension of the SERS measurement (*i.e.* the laser spot) is in the scale of micrometers.

The other possible reason for superior SERS signal on Au-

modified AgNR substrate is the generation of more effective electromagnetic resonance. To further study the plasma resonance prosperities of the substrates, AgNR arrays were prepared without the under layer of silver film, which allowed transmission measurements to be obtained. These AgNR substrates were further modified by Au with GRR following aforementioned protocols. Before Au modification, the AgNR array has a LSPR peak at 383 nm, which can be assigned to its transverse mode. After Au modification, the LSPR peak shifts to longer wavelengths with a broad band centered around 500 nm (ESI† Fig. S8). Such a red-shifted and broadened band overlaps with the LSPR band of the Im-AuNPs (ESI† Fig. S5). As the localized surface plasma resonance of the capture substrate couples well with the AuNPs when irradiated by the same incidence laser beam, a stronger enhancement to the electromagnetic field occurs. According to the results obtained from this SERS immunoassay, the ratio of SERS intensity collected on Au-modified AgNR substrate is approximately 1.4 times greater than that on unmodified AgNR substrate, and the average surface density of AuNPs on the Au-modified substrate is approximately 1.4 times higher than that on unmodified AgNRs. Therefore, we speculate that Au modification with improved capture efficiency of Im-AuNPs is the main reason for the higher sensitivity of immunoassays performed on the Au-modified AgNRs, and the coupling of LSPR between substrate and Im-AuNPs is an unimportant supplement to the improvement.

The limit of detection (LOD) of the SERS immunoassay on the Au-modified AgNRs was determined using a concentration gradient of human-IgGs ranging from 100 fg/mL to 100 ng/mL. The concentration-dependent SERS spectra are shown in Fig. 5a, in which each curve is averaged from eight SERS scans. It is observed that the intensity of the 1080 cm^{-1} and 1587 cm^{-1} peaks from 4-MBA decreases with the reducing human-IgG concentration. As shown in Fig. 5b, a good linear relationship is found between the peak intensity at 1080 cm^{-1} and the logarithm of human-IgG concentration in the range between 100 fg/mL and 100 ng/mL. The LOD for human-IgG is estimated to be 2.5 fg/mL, as defined by the lowest concentration that produces a signal three times stronger than the standard deviation of the control (*i.e.* BSA) at the 1080 cm^{-1} 4-MBA peak. A comparison with the reported sandwich structured SERS immunoassays for IgG is summarized in Table S1 (ESI†).

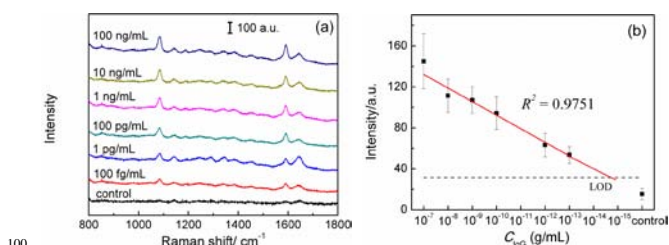


Fig. 5 (a) SERS spectra of target human-IgG in the sandwich immunoassay at different concentrations. (b) Linear fitting of the peak intensities at 1080 cm^{-1} as a function of the logarithm of human-IgG concentration. Error bars indicate the standard deviation obtained from eight measurements.

4 Conclusions

The work reports a sandwich SERS immunoassay performed on

aligned AgNR and Au-modified AgNR substrates for the first time. The tilted AgNR arrays were deposited on a glass slide by OAD, and modified with Au by the GRR process. SERS characterization indicates a decreased SERS activity of the AgNRs as a result of Au modification. However, higher detection sensitivity for the SERS immunoassay was achieved using the Au-modified substrate (approximately 1.4 times as strong as that obtained on the bare AgNR substrates). Such an enhanced SERS signal can be reasonably attributed to the increased number and uniformity of captured Im-AuNPs on the substrate and the improved LSPR coupling between the Au-modified AgNR substrate and the Im-AuNPs. The average surface density of Im-AuNPs on the Au-modified substrate is approximately 1.4 times higher than that on the un-modified AgNRs, which coincides with the ratio in observed SERS intensities. The concentration-dependent SERS spectra indicate a good linear relationship between the SERS response and the logarithm of the human-IgG concentration in the concentration range from 100 fg/mL to 100 ng/mL, and the LOD is determined to be as low as 2.5 fg/mL. This immuno-SERS assay demonstrates a potential for highly specific SERS detection with improved detection sensitivity due to the use of Au-modified AgNR substrates, and could be employed in the detection of a variety of detection targets from complicated matrices, such as pathogenic species and disease biomarkers from clinical specimens.

Acknowledgements

This work was supported by the National Key Basic Research Program of China (973) (2012CB933301), National Natural Science Foundation of China (61302027), Natural Science Foundation Of Jiangsu Province (BK20130871), Program for Changjiang Scholars and Innovative Research Team in University (IRT1148), Sci-tech Support Plan of Jiangsu Province (BE2014719) and the Open Research Fund of State Key Laboratory of Bioelectronics, Southeast University. A Project Funded by the Priority Academic Program Development of Jiangsu Higher Education Institutions (PAPD). Y.-P.Z would like to acknowledge the financial support from National Science Foundation under contract number CBET-1064228. The authors thank Dr. Justin L. Abell and Mr. Layne H. Bradley for proofreading the manuscript.

Notes

^a Key Lab Organic Electronics & Information Displays (KLOEID), Institute of Advanced Materials (IAM), and Synergetic Innovation Center for Organic Electronics and Information Displays, Nanjing University Posts & Telecommunications, Nanjing 210023, China. E-mail: iamcysong@njupt.edu.cn; iamhlwang@njupt.edu.cn

^b Department of Physics and Astronomy, University of Georgia, Athens, Georgia 30602, USA

^c Nanoscale Science and Engineering Center, University of Georgia, Athens, Georgia 30605, USA

^d Department of Food Science and Technology, University of Georgia, Athens, Georgia 30602, USA

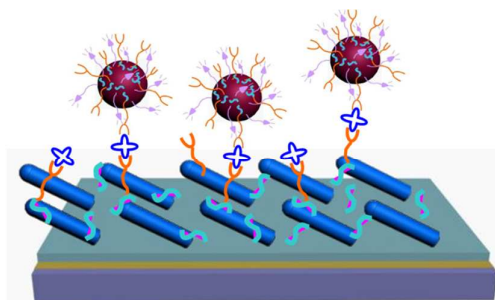
[†] Electronic Supplementary Information (ESI) available: Supplementary figures. See DOI: 10.1039/b000000x/

References

- H. Zhang, M. H. Harpster, H. J. Park and P. A. Johnson, *Anal. Chem.*, 2011, **83**, 254-260.
- G. F. Wang, R. J. Lipert, M. Jain, S. Kaur, S. Chakraborty, M. P. Torres, S. K. Batra, R. E. Brand and M. D. Porter, *Anal. Chem.*, 2011, **83**, 2554-2561.
- K. R. Wigginton and P. J. Vikesland, *Analyst*, 2010, **135**, 1320-1326.
- H. Chon, S. Lee, S. Y. Yoon, E. K. Lee, S. I. Chang and J. Choo, *Chem. Commun.*, 2014, **50**, 1058-1060.
- G. Lu, H. Li, C. Liusman, Z. Yin, S. Wu and H. Zhang, *Chem. Sci.*, 2011, **2**, 1817-1821.
- G. Lu, H. Li, S. Wu, P. Chen and H. Zhang, *Nanoscale*, 2012, **4**, 860-863.
- G. Lu, H. Li and H. Zhang, *Chem. Commun.*, 2011, **47**, 8560-8562.
- G. Lu, H. Li and H. Zhang, *Small*, 2012, **8**, 1336-1340.
- J. Ni, R. J. Lipert, G. B. Dawson and M. D. Porter, *Anal. Chem.*, 1999, **71**, 4903-4908.
- M. Lee, S. Lee, J. H. Lee, H. W. Lim, G. H. Seong, E. K. Lee, S. I. Chang, C. H. Oh and J. Choo, *Biosens. Bioelectron.*, 2011, **26**, 2135-2141.
- E. J. Dufek, B. Ehlert, M. C. Granger, T. M. Sandrock, S. L. Legge, M. G. Herrmann, A. W. Meikle and M. D. Porter, *Analyst*, 2010, **135**, 2811-2817.
- C. C. Lin, Y. M. Yang, Y. F. Chen, T. S. Yang and H. C. Chang, *Biosens. Bioelectron.*, 2008, **24**, 178-183.
- P. Douglas, R. J. Stokes, D. Graham and W. E. Smith, *Analyst*, 2008, **133**, 791-796.
- B. Guven, N. Basaran-Akgul, E. Temur, U. Tamer and I. H. Boyaci, *Analyst*, 2011, **136**, 740-748.
- X. Su, J. Zhang, L. Sun, T. W. Koo, S. Chan, N. Sundararajan, M. Yamakawa and A. A. Berlin, *Nano Lett.*, 2005, **5**, 49-54.
- K. Kim, H. B. Lee, J. Y. Choi and K. S. Shin, *ACS Appl. Mater. Inter.*, 2011, **3**, 324-330.
- C. G. Wang, Y. Chen, T. T. Wang, Z. F. Ma and Z. M. Su, *Adv. Funct. Mater.*, 2008, **18**, 355-361.
- H. Chon, C. Lim, S. M. Ha, Y. Ahn, E. K. Lee, S. I. Chang, G. H. Seong and J. Choo, *Anal. Chem.*, 2010, **82**, 5290-5295.
- C. Y. Song, Z. Y. Wang, J. Yang, R. H. Zhang and Y. P. Cui, *Colloid. Surf. B: Biointerfaces*, 2010, **81**, 285-288.
- Z. Wang, S. Zong, W. Li, C. Wang, S. Xu, H. Chen and Y. Cui, *J. Am. Chem. Soc.*, 2012, **134**, 2993-3000.
- C. Y. Song, Z. Y. Wang, R. H. Zhang, J. Yang, X. B. Tan and Y. P. Cui, *Biosens. Bioelectron.*, 2009, **25**, 826-831.
- X. X. Han, Y. Kitahama, T. Itoh, C. X. Wang, B. Zhao and Y. Ozaki, *Anal. Chem.*, 2009, **81**, 3350-3355.
- Y. W. Pei, Z. Y. Wang, S. F. Zong and Y. P. Cui, *J. Mater. Chem. B*, 2013, **1**, 3992-3998.
- J. D. Driskell, S. Shanmukh, Y. Liu, S. B. Chaney, X. J. Tang, Y. P. Zhao and R. A. Dluhy, *J. Phys. Chem. C*, 2008, **112**, 895-901.
- J. L. Abell, J. D. Driskell, R. A. Dluhy, R. A. Tripp and Y. P. Zhao, *Biosens. Bioelectron.*, 2009, **24**, 3663-3670.
- J. L. Abell, J. M. Garren, J. D. Driskell, R. A. Tripp and Y. Zhao, *J. Am. Chem. Soc.*, 2012, **134**, 12889-12892.
- C. Y. Song, J. L. Abell, Y. P. He, S. H. Murph, Y. P. Cui and Y. P. Zhao, *J. Mater. Chem.*, 2012, **22**, 1150-1159.

-
28. Y. J. Liu, H. Y. Chu and Y. P. Zhao, *J. Phys. Chem. C*, 2010, **114**, 8176-8183.
29. G. Frens, *Nature*, 1973, **241**, 20-22.
30. Y. G. Sun and Y. N. Xia, *J. Am. Chem. Soc.*, 2004, **126**, 3892-3901.
- 5 31. M. Erol, Y. Han, S. K. Stanley, C. M. Stafford, H. Du and S. Sukhishvili, *J. Am. Chem. Soc.*, 2009, **131**, 7480-7481.
32. K. L. Kelly, E. Coronado, L. L. Zhao and G. C. Schatz, *J. Phys. Chem. B*, 2003, **107**, 668-677.
33. W.-C. Law, K.-T. Yong, A. Baev and P. N. Prasad, *ACS Nano*, 2011, 10 **5**, 4858-4864.
34. N. T. K. Thanh and Z. Rosenzweig, *Anal. Chem.*, 2002, **74**, 1624-1628.
35. C. Y. Song, Z. Y. Wang, J. Yang, R. H. Zhang, X. B. Tan and Y. P. Cui, *Acta Chim. Sinica*, 2009, **67**, 493-498.
- 15 36. C. Y. Song, J. Chen, J. L. Abell, Y. P. Cui and Y. P. Zhao, *Langmuir*, 2012, **28**, 1488-1495.
37. Y. P. Zhao, S. B. Chaney and Z. Y. Zhang, *J. Appl. Phys.*, 2006, **100**, 063527.
38. Y. Li and Z. Ma, *Nanotechnology*, 2013, **24**, 275605.
- 20 39. L. Wu, Z. Y. Wang, S. F. Zong, Z. Huang, P. Y. Zhang and Y. P. Cui, *Biosens. Bioelectron.*, 2012, **38**, 94-99.

Graphical Abstract



Silver nanorod arrays and Au-modified AgNR arrays are fabricated for SERS immunoassays and an improved sensitivity is obtained.